

Strain-Dependent Electrical Properties of a Conductive MWCNT/PEO Composite Film

Myounggu Park* and Hyonny Kim**

* Purdue University, School of Aeronautics and Astronautics

** University of California San Diego, Department of Structural Engineering

Keywords: *Multiwalled Carbon Nanotube/ Poly Ethylene Oxide composite, Electrical Resistance and strain relationship, Strain Sensor*

Abstract

Multiwalled carbon nanotubes (MWCNT) were combined with polyethylene oxide (PEO) to make a series of conductive MWCNT/PEO composite films containing different volume fractions of MWCNT. Samples from the different loadings of MWCNT were bonded onto the surface of a dogbone-shaped polycarbonate substrate. This substrate allowed the film to be stretched through a large strain range (0.07) using a conventional uniaxial test machine. Unique and repeatable relationships in resistance versus strain were obtained for multiple samples with different volume fractions of MWCNT. The overall pattern of electrical resistance change versus strain for the samples of each volume fraction of MWCNT consists of linear and non-linear regions. A model to describe the combination of linear and non-linear modes of electrical resistance change as a function of strain is suggested. The unique characteristics in electrical resistance change for different volume fractions implies that nanotube composites can be used as tunable strain sensors for application into embedded sensor systems in structures.

1 Introduction

Electromechanical behavior of carbon nanotube/polymer composites is closely related to smart structures research, such as sensor/actuators embedded in the composite structure for enhancing performance and monitoring health [1, 2]. Among the many functions being pursued, strain sensing is one of the most basic ones, which needs the fundamental understanding of the electromechanical behavior of CNT/polymer composite materials. Recently, a large body of research about carbon

nanotube (CNT) embedded polymer composites under straining has been conducted [3, 4]. However, fundamental mechanism of electrical resistance change of CNT embedded polymer under strain is not yet fully understood. Also, the understanding of this mechanism is indispensable for the proper and effective application of CNT composite film as sensors. Thus, the topic of this paper is focused on the physical understanding of electrical resistance change in CNT composite films.

2 Experiments

Fabrication of MWCNT/PEO composite film and determination of the percolation threshold are described in ref. [5]. To investigate the relationship between electrical resistance and strain for a composite sample near the percolation threshold, two different volume fractions were tested: 0.56 and 1.44 vol% of MWCNT. From each volume fraction, two samples were chosen. Details of the measurement setup are shown in Fig. 1. A dogbone-shaped polycarbonate tensile test specimen was prepared and the MWNT/PEO composite film strips of 0.56 and 3.2 vol% MWCNT were bonded onto the center of the gage section using adhesive (M Bond 200) as shown in Fig. 2. The polycarbonate substrate has gage section dimensions of 60 by 30 mm, and thickness 2.92 mm. The test specimen was stretched using a uniaxial test machine (MTS 810). The strain of the combined sample was recorded using a laser extensometer (Electronics Instrument Research, Model LE-05) while the resistance of the MWCNT/PEO film was simultaneously measured using the precision multimeter. Since the MWCNT/PEO film is well bonded to the substrate and has much lower stiffness, the strain in the film is the same as the strain in the polycarbonate substrate.

To make sure that the resistance change was induced only by the deformation of the composite film, the end regions of the film were not bonded onto the dogbone specimen and the lead wires were then attached to these free end surfaces (see Fig. 2) using the method described in ref [5].

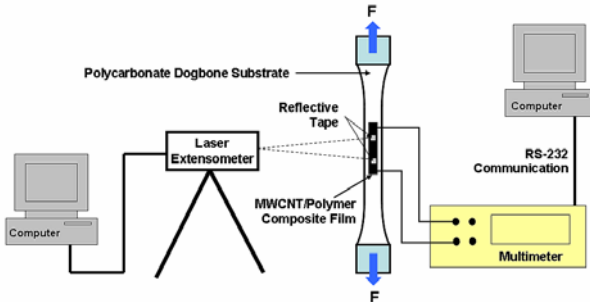


Fig. 1. Electrical Resistance and Strain Measurement Setup

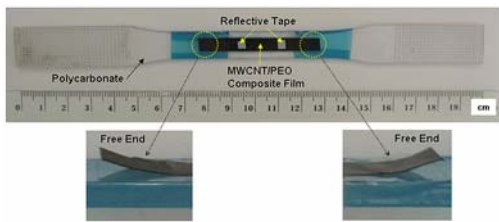


Fig. 2. Detailed View of Detached Film Free Ends

3 Experimental Results

The initial electrical resistances were 598 and 493 K Ω for the two samples having 0.56 vol% of MWCNT and 6.89 and 6.29 K Ω for the samples having 1.44 vol% of MWCNT. To compare the relationship between electrical resistance versus strain, the change in electrical resistance $\Delta R/R_0$ is plotted against strain in Figs. 3 and 4 where ΔR is the difference between current resistance (R) and initial resistance (R_0). For the MWCNT 0.56 vol% films (see Fig. 3), the electrical resistance increased in linear and monotonic manner up to 0.008 strain, and then it transitioned to a non-linear behavior: it made sudden jump in electrical resistance just before 0.009 strain. For the MWCNT 1.44 vol% films (see Fig. 4), electrical resistance increased linearly over a larger strain range (0.02) compared to the MWCNT 0.56 vol% case. After 0.02 strain, the relationship between electrical resistance changed from linear to non-linear behavior. The measurements were stopped due to the onset of the localized necking of the polycarbonate dogbone tensile specimen at about 0.07 strain. The relationship between electrical resistance and strain can be divided into two regions:

linear and non-linear for both the 0.56 and 1.44 vol% cases (see Figs. 3 and 4). The linear and non-linear region was more distinctive for MWCNT 0.56 vol% samples compared with those of MWCNT 1.44 vol%. However, the overall pattern of electrical resistance change versus strain for the samples of each volume fraction of MWCNT was repeatable within a reasonable manner. The reasons for the combination of linear and non-linear modes of electrical resistance change as a function of strain is discussed in the following sections.

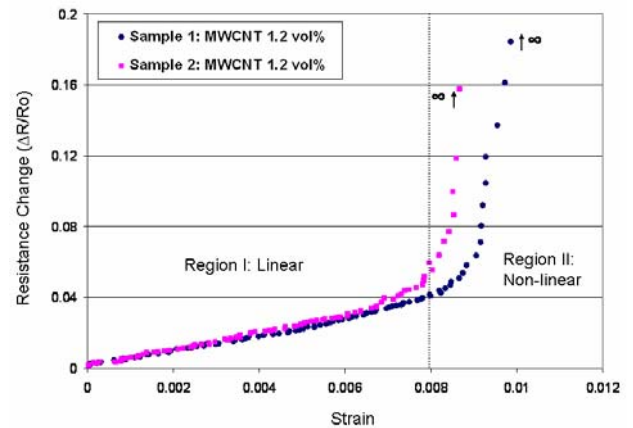


Fig. 3. Resistance vs. Strain for 0.56 vol% of MWCNT

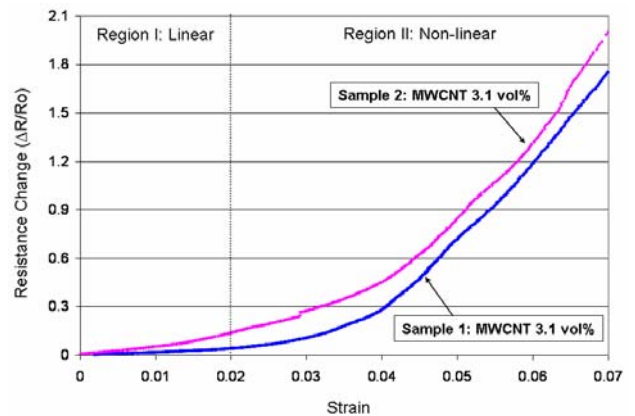


Fig. 4. Resistance vs. Strain for 1.44 vol% of MWCNT

4 Electrical Resistance vs. Microstructure

As a MWCNT/PEO composite sample is stretched, the initial microstructure of the material changes thereby affecting the MWCNT-to-MWCNT contacts, a result of the random network of MWCNT becoming ordered. The microstructure change of a 5.9 vol% sample was directly observed before and after straining by field-emission scanning electron microscope (FE-SEM). The amount of strain applied

to the sample was approximately 100% which is much larger than the levels shown in Figs. 1 and 2 in order to obtain better observation. As shown in Figs. 5 and 6, when the sample is stretched, initially nondirectionally embedded MWCNTs become straight and aligned in the direction of stretching (see MWCNTs pointed out in Fig. 6b). The severity in the loss of contact from the initial contact state during straining can result in different modes of macroscopic electrical resistance change. It is conjectured that for a sample well above percolation threshold the loss of contacts is less severe than a sample near the percolation threshold under the same amount of applied strain. Thus by varying the volume fraction of MWCNT, unique strain dependent electrical resistance change can be obtained.

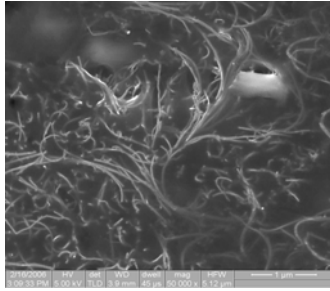
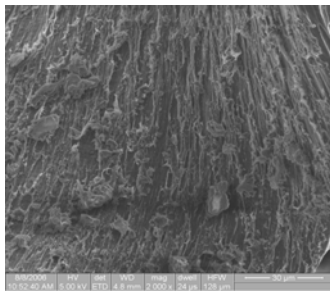
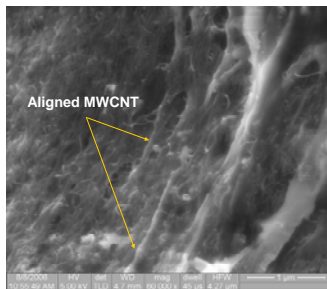


Fig. 5. Microstructure of MWCNT/PEO Composite before Straining



(a) Overall View



(b) Closeup View

Fig. 6. Microstructure of MWCNT/PEO Composite after Straining

5 Parameters Affecting Electrical Resistance

Mirostructure change of a sample due to large tensile strain indicated a qualitative rationale for the electrical resistance change of MWCNT/PEO composite film. In this section, to further understand the electrical resistance change mechanisms, four parameters were considered and analyzed: volume change of the sample, angle change of individual CNT, electrical property change of individual CNT itself, and tunneling distance between CNTs. In the following analyses, CNTs were assumed as having rod-like geometry.

5.1 Volume and Angle Change

The influence of volume and angle change on electrical conductivity was studied using a percolation based scaling rule over a strain range of 0.07. Above percolation threshold, it is well known that the electrical conductivity of composites follows the scaling relationship [6, 7, 8]

$$G \propto (\Phi - \Phi_c)^t \quad (1)$$

where G is conductivity, Φ is the volume fraction of CNT, Φ_c is the percolation threshold and t is the conductivity critical exponent. Eq (1) represents the conductivity of a composite sample for different volume fractions of conductive filler near the percolation threshold. In the 3D case, the percolation threshold (Φ_c) can be calculated by the equation given by Balberg [8]

$$\Phi_c = 1 - \exp\left(-\frac{\langle V_{ex} \rangle V}{\langle V_e \rangle}\right) \quad (2)$$

where $\langle V_{ex} \rangle$ is the total excluded volume of a sample and is a constant between 1.4 and 2.8, V is the volume of a CNT and $\langle V_e \rangle$ is the average excluded volume of a CNT and is defined as the volume around a CNT in which the center of another CNT is not allowed to penetrate. Both the total excluded volume and the average excluded volume of CNT are affected by the randomness of CNTs inside the matrix and detailed explanations of these quantities can be found in references [8, 9]. The volume and angle change are the closely related parameters to Eq.(1) affecting Φ and Φ_c .

The normalized volume change of MWCNT/PEO composite bonded onto the substrate under tensile strain in the x direction can be represented by the following equation

$$\frac{V}{V_o} = (1 + \varepsilon_x)(1 - \nu_{xy}\varepsilon_x)(1 - \nu_{xz}\varepsilon_x) \quad (3)$$

where V is the new volume due to tensile strain, V_o is the initial volume of the sample, ε_x is the strain in the x direction, ν_{xy} is the Poisson's ratio of the substrate in the y direction and ν_{xz} is Poisson's ratio of the sample in the z direction, respectively. Volume change is calculated and plotted as a function of strain in Fig. 7 using typical measured sample dimensions. Maximum volume change corresponding to 0.07 strain is calculated as 1.67 percent.

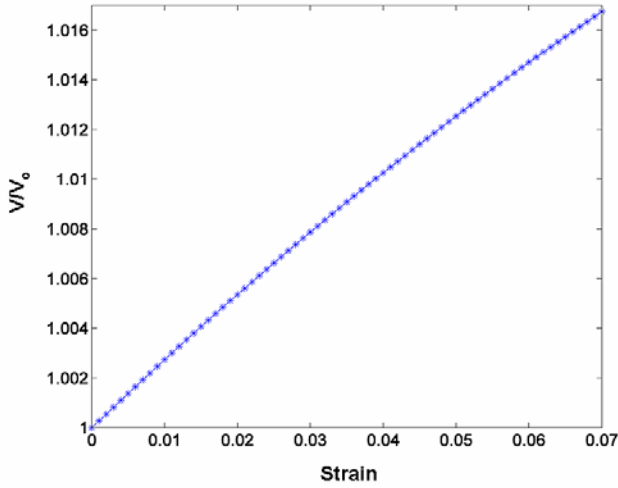


Fig. 7. Volume Change of MWCNT/PEO Composite under Strain

The angles of the CNT inside the matrix also change with respect to the chosen coordinate system under strain. These angles described as θ (azimuthal angle) and α (angle between z axis and CNT) are depicted in Fig. 8. The angle of the CNTs for a strain ε_x inside the matrix changes to align in the direction of strain. The angle change of CNT can be calculated using equations derived by Taya *et al* [10],

$$\theta = \tan^{-1} \left(\frac{(1 - \nu_{xy}\varepsilon_x)}{(1 + \varepsilon_x)} \tan \theta_o \right) \quad (4)$$

$$\alpha = \tan^{-1} \left(\frac{(1 - \nu_{xy}\varepsilon_x) \sin \theta_o}{(1 - \nu_{xz}\varepsilon_x) \sin \theta} \tan \alpha_o \right) \quad (5)$$

where θ is the new azimuthal angle, α is the new angle between z axis and CNT, θ_o is the original azimuthal angle, and α_o is the original angle between the z axis and CNT. The relative angle changes for

both angles are plotted in Fig. 9 for original angles ranging from zero to $\pi/2$ rad.

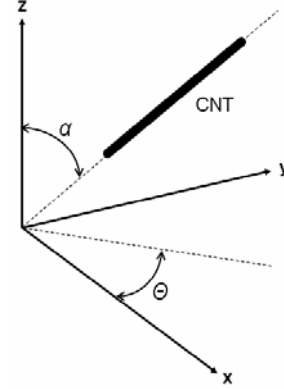
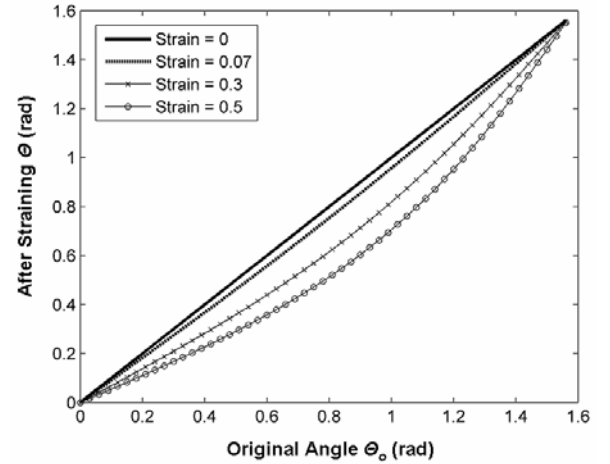
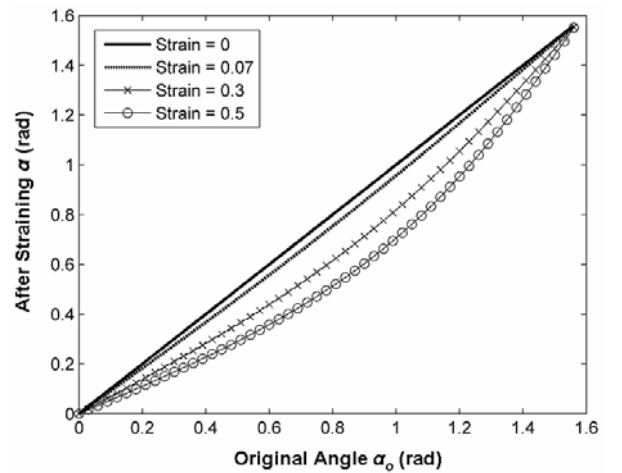


Fig. 8. Angles of CNT in PEO Matrix



(a) Azimuthal Angle Change (θ)



(b) Angle Change between Z-axis and CNT (α)

Fig. 9. Angle Change of CNT in PEO due to Strain

Under tensile strain, the total volume of the composite sample increases and therefore the CNT volume fraction Φ decreases. Also, CNTs tend to align in the direction of external strain and this increases Φ_c due to increase of total excluded volume and the decrease of average excluded volume of CNT in Eq.(2) [8, 9, 11, 12]. Therefore, the net value of $(\Phi - \Phi_c)$ becomes smaller in Eq. (1) and the conductivity G decreases. Φ is inversely linear to volume change and Φ_c is assumed to change linearly with respect to volume change. Note that each increased volume has corresponding increased Φ_c and the angle change is very small with respect to volume (equivalent strain) change. Then Eq. (1) is modified as following:

$$G = K \left[\frac{1}{c} \cdot \Phi - c \cdot \Phi_c \right]^t \quad (6)$$

where K is a constant, c is the V/V_0 calculated by Eq. (3), Φ is the given volume fraction of CNT, Φ_c and t are 0.63 vol.% and 4 respectively. The critical conductivity exponent was calculated by curve fit and it was found to be 4 [13]. $\Delta R/R_0$ vs. strain are plotted in Figs. 10 and 11 for both calculated values using Eq.(6) and experimental data. Overall, the calculated resistance values using Eq. (6) showed linear relationship between $\Delta R/R_0$ and strain and the slopes are calculated as 3.7 for 0.56 vol% and 1.6 for 1.44 vol%. Relatively, they are in good agreement with experimental results over the linear region. However, after passing linear region, the experimental data deviate from the scaling rule predictions.

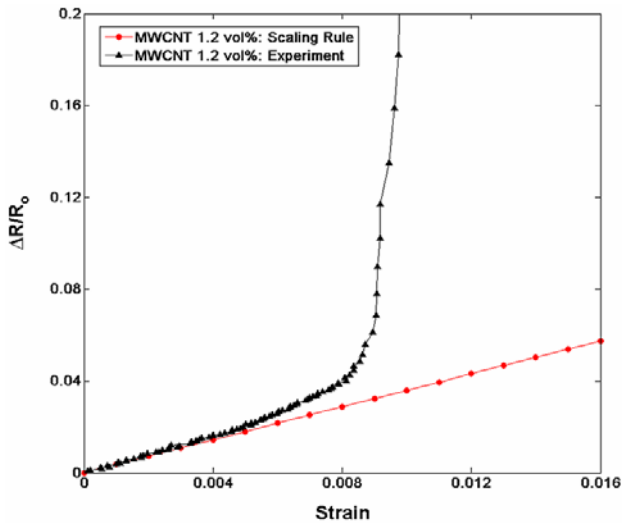


Fig. 10. Resistance Change vs. Strain

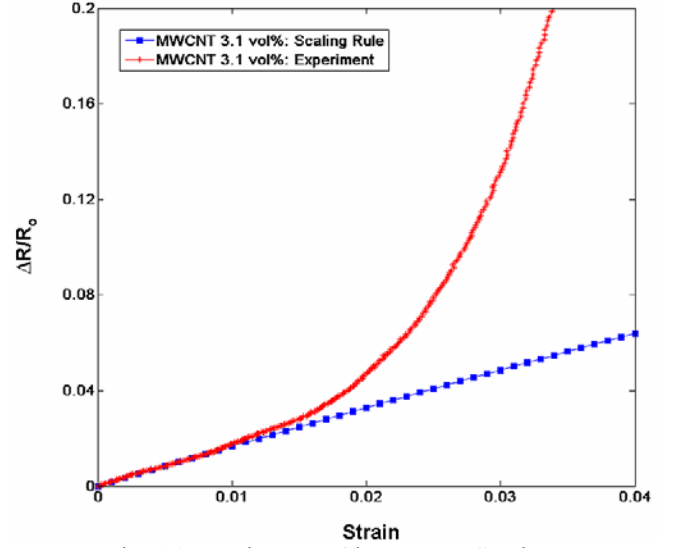


Fig. 11. Resistance Change vs. Strain

5.2 Resistance of Individual CNT

The change of electrical property of an individual CNT is due to the band gap change occurring when external strain is applied. The relationship between band gap change and strain tensor was derived by other researchers [14, 15] and the following is the relationship derived by Kleiner *et al* [14],

$$E_g = \left| \left(\frac{t_o \pi^2}{8c_h^5} + \frac{a_o b \sqrt{3}}{4c_h^3} (\varepsilon_c - \varepsilon_t) \right) \sqrt{3(n-m)(2n^2 + 5mm + 2m^2)} \right| \quad (7)$$

where E_g is the band gap, t_o is the hopping parameter, c_h is the circumference of a CNT, a_o is the length of lattice vector, b is the linear change in the hopping parameter due to change in carbon-carbon bond length, n and m are the components of chiral vector (n, m) , ε_t is the strain along the tube, ε_c is the circumferential strain along the tube. It is also assumed that there is no torsional strain. Eq. (7) provides a guide to understand band gap change of the CNT under axial deformation. For example, a metallic CNT ($n = m$) under axial strain is calculated by Eq.(7) to have no band gap change and remains as metallic always when there is no torsional strain [14, 15]. Another two types of CNT (semimetallic: $n - m = 3q$ and semiconducting: $n - m \neq 3q$ where q is the integer) can be more sensitive to strain and exhibit band gap change [16]. MWCNT consists of multiple numbers of graphene tubes and it can have a combination of effects from band gap change in the numerous tubes. It is known that most MWCNT can be metallic [17]. Electrical resistance of a MWCNT was measured and it was

found that electrical resistance remained unchanged until breakage [17]. Another experimental work reported by Cao *et al* [16] shows that electrical resistance of metallic SWCNT can vary linearly with small finite slope. It is a reasonable assumption that metallic CNTs under applied strain show almost no change in the band gap and thus, the electrical resistance. Therefore, the electrical resistance change of individual MWCNT due to strain can be negligible and the macroscopic electrical resistance is not affected.

5.3 Tunneling Resistance

Carbon nanotubes inside the PEO matrix can be thought of as a network of resistors. The electrical resistance of the network consists of the electrical resistance of the CNT and the tunneling resistance between CNTs. Since the electrical resistance change of an individual MWCNT is negligible under strain as discussed in the previous section, the tunneling resistance is argued to be major parameter affecting the observed non-linear electrical resistance change at higher strain. The tunneling resistance r_1 was derived by Simmons [18, 19] and then, approximated for CNT/polymer composite by Yasuoka *et al* [20] as

$$\frac{r_1}{r_o} \approx \exp\left(\frac{4\pi\sqrt{2m\beta}}{h} s_o [1 + \varepsilon(\cos^2 \eta - \nu \sin^2 \eta)]\right) \quad (8)$$

where r_o is the original tunneling resistance, r_1 is the new tunneling resistance, h is Plank's constant (6.62×10^{-34} Js) [21], m is the mass of an electron (9.11×10^{-31} kg) [21], β is the work function of a CNT (4.8 eV) [22, 23], s_o is the initial distance between CNTs, ε is the applied strain, η is the angle of the conduction path with respect to the axis of applied strain, and ν is Poisson's ratio of CNT. Eq. (8) shows that tunneling resistance varies exponentially with respect to the initial distance (s_o) between CNTs and strain (ε). For higher volume fractions of CNT, the initial distance (s_o) between CNTs is smaller due to closer packing. This can cause different resistance-strain changing behavior compared with films having lower volume fraction. The tunneling resistance change related by the initial distance between CNTs was suitable to describe the non-linear region of the experimental results shown in Figs. 1 and 2.

5.4 Modeling

In the previous sections, it was shown that the linear resistance change region can be related by modified scaling rule, Eq.(6) and non-linear resistance change region by tunneling resistance, Eq. (8). In this section, an empirical model is proposed by superposing these two models for predicting electrical resistance change over a wide strain range. The MWCNTs inside the matrix can generally be considered as overlapping at the contact locations, rather than being arranged in an end-to-end configuration. This contact is highly simplified and depicted in Fig. 12.

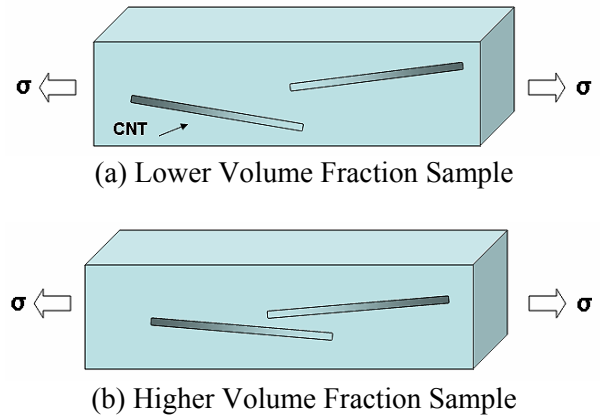


Fig. 12. Contact Geometry of CNTs inside Matrix

Under applied strain, the overall resistance change can be represented by summation of linear and non-linear resistance change contributions. This can be expressed as

$$\frac{\Delta R}{R_o} = \frac{\Delta R_L + \Delta R_N}{R_o} = \frac{\Delta R_L}{R_o} + \frac{\Delta R_N}{R_o} \quad (9)$$

where ΔR_L is resistance change in the linear region, ΔR_N is resistance change in the non-linear region. In the linear region, CNTs are still in contact and the scaling rule is applicable. However, at a critical strain level CNTs begin to separate and no more contact is maintained. Thus, tunneling resistance now becomes important beyond the critical strain defined as ε^c . Using Eq. (6) and Eq. (8), the following equation is proposed for predicting strain dependent resistance of the composite:

$$\frac{\Delta R}{R_o} \approx k \cdot \varepsilon + u(\varepsilon - \varepsilon^c) A \quad (10)$$

where

$$A = \exp\left(\frac{4\pi\sqrt{2m\beta}}{h} \langle s_o \rangle [1 + (\varepsilon - \varepsilon^c) (\cos^2 \langle \eta \rangle - \nu \sin^2 \langle \eta \rangle)]\right) - 1$$

where k is the slope of linear region determined using Eq. (6), and ε^c is the critical strain, $\langle s_o \rangle$ is the average distance between CNTs, and $\langle \eta \rangle$ is the average angle between direction of applied strain and tunneling path. $\langle \eta \rangle$ is calculated as $\langle \eta \rangle = \sin^{-1}(\pi/4)$ [24]. Best fit is obtained when $\langle s_o \rangle$ and ε^c are 300 Å and 0.008 for 0.56 vol% and 50 Å and 0.03 for 1.44 vol% as shown in Fig. 13. Eq. (10) is capable of describing strain dependent resistance reasonably well except at the transition region near the critical strain.

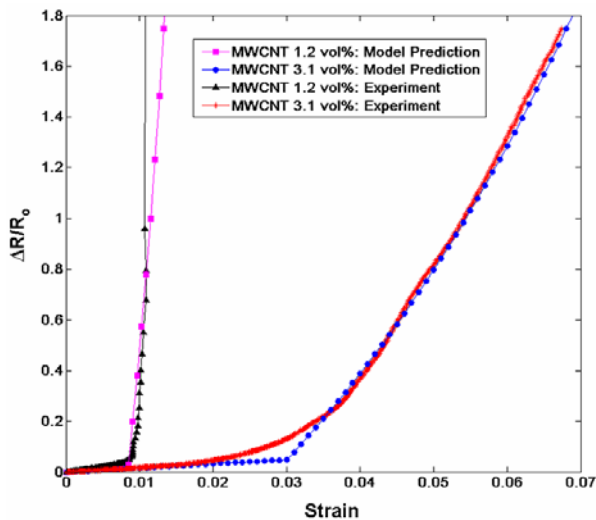


Fig. 13. Resistance Change vs. Strain Relation Predicted using Proposed Model

6 Conclusions

Unique and repeatable relationships between electrical resistance and strain for different volume fractions of MWCNT were observed. The overall pattern of electrical resistance change versus strain for the samples of each volume fraction of MWCNT consists of linear and non-linear regions. In linear region, percolation theory-based scaling rule predictions matched well with experimental results but breaks down at the non linear region. In the non-linear region, tunneling resistance is argued to be a major parameter affecting the macroscopic electrical resistance of the MWCNT/PEO film. A model combining scaling rule and tunneling resistance can predict the linear and non-linear modes of electrical

resistance over a wide range of strain. The high strain sensitivity and repeatable characteristics in electrical resistance change of the MWCNT/PEO films permit these materials to be used as strain sensors for application into smart structure systems.

7 Acknowledgements

This research was supported by Purdue Research Foundation.

8 References

- [1] Blanas P and Das-gupta DK. "Composite Piezoelectric Sensors for Smart Composite Structures". *10th International Symposium on Electrets*, pp. 731-734, 1999.
- [2] Javidinejad A and Joshi SP. "Design and structural testing of smart composite structures with embedded conductive thermoplastic film". *Smart Mater Struct*, vol. 8, pp. 585-90, 1999.
- [3] Frogley MD, Zhao Q and Wagner HD. "Polarized resonance Raman spectroscopy of single-walled carbon nanotubes within a polymer under strain". *Phys Rev B*, Vol. 65, pp. 113413-1 – 4, 2002.
- [4] Dharap P, Li Z, Nagarajaiah S and Barrera EV. "Nanotube film based on single-wall carbon nanotubes for strain sensing". *Nanotechnology* Vol. 15, pp.379-82, 2004.
- [5] Park M and Kim H. "Evaporation-Based Method for Fabricating Conductive MWCNT/PEO Composite Film and Its Application as Strain Sensor". *12th US-Japan Conference on Composite Materials*, Dearborn, Michigan, paper number 1012, 2006.
- [6] Stauffer D and Aharony A. "Introduction to Percolation Theory". 2nd Edition. New York, CRC press, 1994.
- [7] Munson-McGee SH. "Estimation of the critical concentration in an anisotropic percolation network". *Phys Rev B*, Vol. 43, pp. 3331-36, 1991.
- [8] Balberg I. "Excluded-volume explanation of Archie's law". *Phys Rev B*, Vol. 33, pp. 3618 – 20, 1986.
- [9] Balberg I, Anderson CH, Alexander S and Wagner N. "Excluded volume and its relation to the onset of percolation". *Phys Rev B*, Vol. 30, pp. 3933 – 43, 1984.
- [10] Taya M, Kim WJ and Ono K. "Piezoresistivity of a short fiber/elastomer matrix composite". *Mech Mater*, Vol. 28, pp. 53 – 9, 1998.
- [11] Balberg I, Binenbaum N and Wagner N. "Percolation thresholds in the three-dimensional sticks system". *Phys Rev Lett*, Vol. 52, pp. 1465 – 86, 1984.
- [12] Balberg I. "Universal percolation-threshold limits in the continuum". *Phys Rev B*, Vol.31, pp.4053 – 55, 1985.

- [13] Park M. “*Deformation Dependent Electrical Resistance of Multiwalled Carbon Nanotube/PEO Composite Films*”, Ph.D. Thesis, School of Aeronautics and Astronautics, Purdue University, 2007. (in preparation)
- [14] Kleiner A and Eggert S. “Band gaps of primary metallic carbon nanotubes”. *Phys Rev B*, Vol. 63, pp.073408-1 –4. 2001.
- [15] Yang L, Anantram MP, Han J and Lu JP. “Band-gap change of carbon nanotubes: Effect of small uniaxial and torsional strain”. *Phys Rev B*, Vol.60, pp. 13 874 – 78, 1999.
- [16] Cao J, Wang Q and Dai H, “Electromechanical Properties of Metallic, Quasimetallic, and Semiconducting Carbon Nanotubes under Stretching”. *Phys Rev Lett*, Vol. 85, pp.157601-1-4, 2000.
- [17] Paulson S, Falvo MR, Snider N, Helser A, Hudson T, Seeger A, Taylor RM, Superfine R and Washburn S, “In Situ resistance measurements of strained carbon nanotubes”. *Appl Phys Letts*, Vol.75, pp. 2933 – 38. 1999.
- [18] Simmons JG. “Low-Voltage Current-Voltage Relationship of Tunnel Junctions”. *J Appl Phys*, Vol. 34, pp. 238-9, 1963.
- [19] Simmons JG. “Generalized Formula for the Electric Tunnel Effect between Similar Electrodes Separated by a Thin Insulating Film”. *J Appl Phys*, Vol. 34, pp. 1793 – 1803, 1963.
- [20] Yasuoka T, Shimamura Y and Todoroki A. “Piezoresistivity of Carbon-Nanotube Composite”. *The Ninth Japan International SAMPE symposium*, pp. 341- 4, 2005.
- [21] Ashcroft NW and Mermin ND. “*Solid State Physics*”. Thomson Learning, 1976.
- [22] Masashi S and Masafumi A. “Work function of carbon nanotubes”, *Carbon*, Vol. 39, pp. 1913-17, 2001.
- [23] Gao R, Pan Z, Wang ZL. Work function at the tips of multiwalled carbon nanotubes, *Appl Phys Letts*, 2001:78(12):1757-59
- [24] Onsager L. “The effects of shape on the interaction of colloidal particles”. *Ann NY Acad Sci*, Vol.51, pp. 627-59, 1949.